Journal of Nuclear Materials 390–391 (2009) 486–489

Contents lists available at ScienceDirect

Journal of Nuclear Materials

journal homepage: www.elsevier.com/locate/jnucmat

Experimental comparison of recycling and pumping changes during resonant magnetic perturbation experiments at low and high collisionality in DIII-D

E.A. Unterberg [a,*], N.H. Brooks [b], T.E. Evans [b], M.E. Fenstermacher [c], D.L. Hillis [d], R. Maingi [d], S. Mordijck [e], R.A. Moyer [e], T.H. Osborne [b], T.W. Petrie [b], J.G. Watkins [f]

[a] Oak Ridge Institute for Science and Education, P.O. Box 117, Oak Ridge, TN 37831, USA
[b] General Atomics, P.O. Box 85608, San Diego, CA 92186-5608, USA
[c] Lawrence Livermore National Laboratory P.O. Box 808, Livermore, CA 94551, USA
[d] Oak Ridge National Laboratory, P.O. Box 2008, Oak Ridge, TN 37831, USA
[e] University of California-San Diego, 9500 Gilman Drive, La Jolla, CA 92093, USA
[f] Sandia National Laboratory, P.O. Box 5800, Albuquerque, NM 87185, USA

ARTICLE INFO

PACS:
52.25.Xz
52.55.Fa
52.70.Nc
52.25.Fi

ABSTRACT

Resonant magnetic perturbations (RMPs) have been shown to successfully suppress edge localized modes (ELMs) in the DIII-D tokamak. A previous study of target plate conditions highlighted differences in RMP discharges between low and high electron collisionality, ν_e^*, operation in DIII-D. This paper reports on a systematic study of the electron density pump-out associated with the turn-on of the RMP over a wide range of operating conditions in DIII-D, including shapes and collisionalities similar to those anticipated in ITER. It is shown that the pump-out magnitude, Δn_e, has an upper envelope that is inversely proportional to the pedestal ν_e^*. The particle decay times, which are calculated based on global D_2 particle balances, show an increase as the pedestal ν_e^* is increased. Both results are suggestive that the underlying physics mechanism is an increase in edge particle transport and/or that wall depletion is playing a role in the pump-out magnitude.

1. Introduction

Large edge localized modes (ELMs) are expected to have detrimental effects on the first wall of any next step fusion tokamak device (e.g. ITER) [1]. One technique to mitigate large ELMs (e.g. Type-I) is the application of resonant magnetic perturbations (RMPs) to stochastize the magnetic flux surfaces near the edge of the tokamak plasma. This technique successfully mitigates and/or suppresses Type-I ELMs in the DIII-D tokamak [2,3]. RMP discharges with successful ELM mitigation and/or suppression in DIII-D are accompanied by a decrease in plasma density, n_e, which could be unfavorable in future burning-plasma devices if the density were not restored to the design value with core fueling. Therefore, an understanding of the density pump-out is necessary for this technique to translate to burning-plasma devices.

In an effort to understand and quantify the density drop, this paper focuses on the electron density pump-out during RMPs in H-mode, DIII-D plasmas. It has been shown in other tokamak devices that an enhancement in core plasma particle transport occurs with the application of a stochastic boundary [4,5]. Here, we report on a systematic study of the n_e pump-out associated with the turn-on of the RMP over a wide range of operating conditions, including shapes and collisionalities similar to those anticipated in ITER. Two notable differences between these and the ITER scenarios are that the DIII-D experiments were conducted in low-density, attached plasmas, and with strongly pumping walls. The scenarios in ITER will entail partially detached divertor operation with possibly saturated, non-pumping wall.

The remainder of the paper defines techniques to characterize the density pump-out and applies these techniques to an extensive RMP discharge database developed for DIII-D, and possible physical mechanisms to interpret this pump-out characterization are also suggested.

2. Characterization of RMP electron density pump-out

2.1. Experimental setup and technique

For this study a database containing 91 RMP discharges in DIII-D is established. The database spans a range of discharges with varying triangularities ($0.35 < \delta < 0.6$), pedestal electron collisionalities ($0.1 < \nu^*_{e(ped)} < 1$), as defined in the next section, normalized betas ($1.5 < \beta_N < 3$), and Greenwald density fractions,

* Corresponding author. Present address: Oak Ridge Institute for Science and Education, c/o General Atomics, MS 13-368, P.O. Box 85608, San Diego, CA 92186, USA.
E-mail address: unterberge@fusion.gat.com (E.A. Unterberg).

0022-3115/$ - see front matter © 2009 Elsevier B.V. All rights reserved.
doi:10.1016/j.jnucmat.2009.01.052

$f_{GW} = n_e/n_{GW}$ [6] ($0.2 < f_{GW} < 0.7$). Details of several of these discharges are discussed in Refs. [3,7–10].

A typical time history for an RMP discharge in DIII-D is shown in Fig. 1. For all RMP shots in this study, there is a clear density drop as measured by a CO_2 laser interferometer and edge Thomson scattering (TS) system. The drop is illustrated in Fig. 1(b) at ~2.25 s and is coincident with the activation of the RMP, labeled I_{coil} in Fig. 1(a). The discharge has a $\beta_N \approx 2.8$ and $\bar{\delta} \approx 0.54$ at the start of the pump-out phase both of which are on the high end of the database parameters. ELMs are fully suppressed ~150 ms after the I_{coil} turns on, as shown in Fig. 1(c) by the D_α signal from the outer strike point (OSP). The initial fast n_e drop that lasts ~150 ms is typical for most DIII-D, RMP discharges, and is referred to as the density pump-out time in this paper. After this time, the n_e varies slowly until the I_{coil} is turned off, at ~4.5 s, at which time the density recovers. To note, the slow increase in density and D_α signal starting at ~3.25 s is due to a sweep of the OSP away from the cryo-pump baffles and through the D_α viewing chord.

The initial fast n_e drop is characterized in the full set of database discharges by the pump-out magnitude, Δn_e ($= n_{e\_max} - n_{e\_min}$), where n_{e_max} is the density before the perturbation is applied and n_{e_min} is the density after equilibration. Specifically, the n_e decay is fit to a decaying exponential function, from which the maximum n_e, minimum n_e, and density decay time, τ, are obtained.

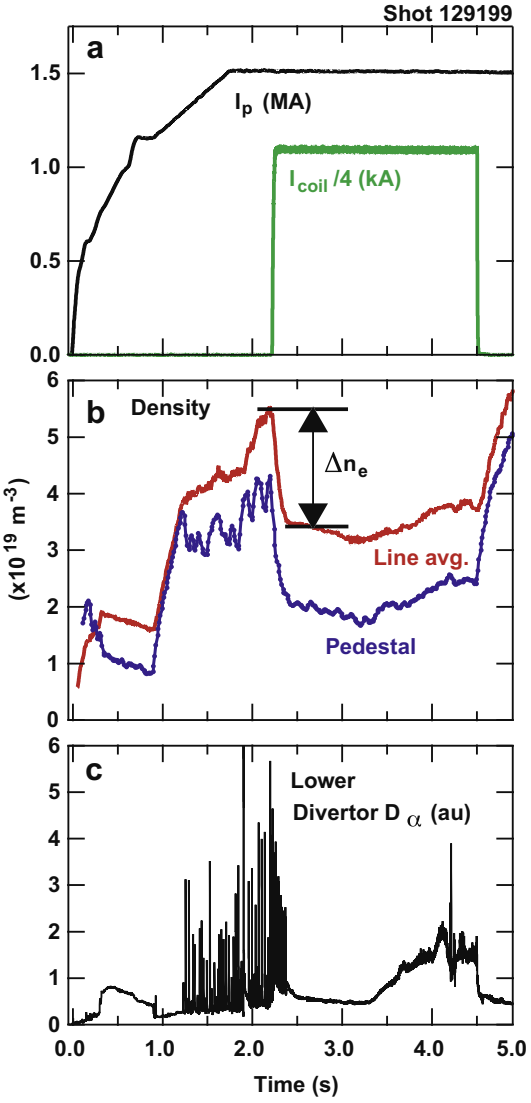

Fig. 1. (a) Plasma current, I_p, and RMP perturbation strength as denoted by the I_{coil} current, (b) density as measured by a CO_2 laser interferometer (labeled line avg.) and edge TS array (labeled pedestal) showing a large density drop (Δn_e) when the I_{coil} turns on and (c) lower divertor D_α signal from the OSP.

Insight into the source and sink terms is obtained with a D_2 global particle balance. The balance is given as: $S_{wall} = S_{IN} - dN_e/dt - Q_{cryo} - dN_0/dt$, where S_{IN} is the sum of the input rates from the gas puff (S_{gas}) and the neutral beam (S_{NBI}), dN_e/dt is the rate change in core plasma electron inventory, Q_{cryo} is the pumping exhaust rate of the DIII-D cryo-system, and dN_0/dt is the rate of change in inventory of non-pumped gaseous neutrals contained under the divertor baffles [11]. The effects of impurities are ignored in this particular study as recent data has shown that impurity content is low ($Z_{eff} \leqslant 2$) for times around the initial RMP turn-on in most discharges [7]. Fig. 2 shows the component rates for a typical particle balance in an RMP discharge. The change in total electrons within the plasma as measured by a CO_2 laser interferometer chord near the magnetic axis is shown in Fig. 2(a). In Fig. 2(b), the input rate of D_2, S_{IN}, and total number of input particles from both gas values and neutral beam injection is given. In Fig. 2(c), the total exhaust rate and total particles exhausted from the three cryo-pumps in DIII-D are given as measured by neutral pressure gauges in the divertor baffles. Finally, the difference of these sources and sinks is shown in Fig. 2(d). While this is interpreted as the change in the wall loading (S_{wall}) and seems to be valid for most discharges in the database, we note that changes in the scrape-off layer (SOL) and divertor particle content could also explain some of the behavior seen, although such changes are more difficult to quantify.

This analysis shows that wall loading could be playing a role in the density drop during the RMP. Firstly, there is a marked influx of particles into the wall during the initial phases of the discharge (0–1 s). Then, during the H-mode transition, there is a depletion of the wall, usually termed outgassing. These first two characteristics are typical of most H-mode discharges on DIII-D [11,12]. When the RMP turns on at 2.25 s, there is an influx of particles into the wall/SOL which amounts to $\sim 2.1 \times 10^{21}$ particles(#)/s for ~0.25 s. Although the exhaust rate to the cryo-pump increases 20–30% at this time, from $\sim 5.6–7 \times 10^{20}$ #/s to $\sim 8.4 \times 10^{20}$ #/s, this does not balance the particle outflux from the core plasma. Therefore, we conclude that the excess particles are going in the wall and/or the SOL/divertor plasma, which is corroborated by an increase in baseline D_α signal denoting an increase in wall recycled D_2 neutrals [e.g. Fig. 1(c) at 2.25 s].

2.2. Comparisons of discharges in database

The pump-out magnitude from the database is now compared to a few global discharge parameters to evaluate possible trends. A notable correlation was found between the pump-out density measured at the top of the pedestal and the pedestal electron collisionality, $\nu^*_{e(ped)}$ [$\equiv Rq_{95}\varepsilon^{-3/2}(\lambda_e)^{-1}$, where R is the major radius, ε is the inverse aspect ratio, and λ_e is the electron mean free path]. Fig. 3 shows that the envelope of the pump-out magnitude decreases as $\nu^*_{e(ped)}$ increases. We note there are also distinct differences in other edge diagnostic parameters at high- and low-$\nu^*_{e(ped)}$ [8,10]. The variability in Δn_e with $\nu^*_{e(ped)}$ is difficult to quantify experimentally due to the many mechanisms potentially influencing the edge particle transport. Changes in the magnetic topology from the RMP can affect the edge particle transport (e.g. particle drift motion or anomalous transport) as well as boundary/SOL conditions (e.g. through changes in neutral ionization physics or recycling sources and sinks) both of which change depending on the collisionality [5]. Although there have been recent attempts to explain the transport observations on DIII-D H-mode discharges during the application of an RMP, a full understanding is still under investigation [13].

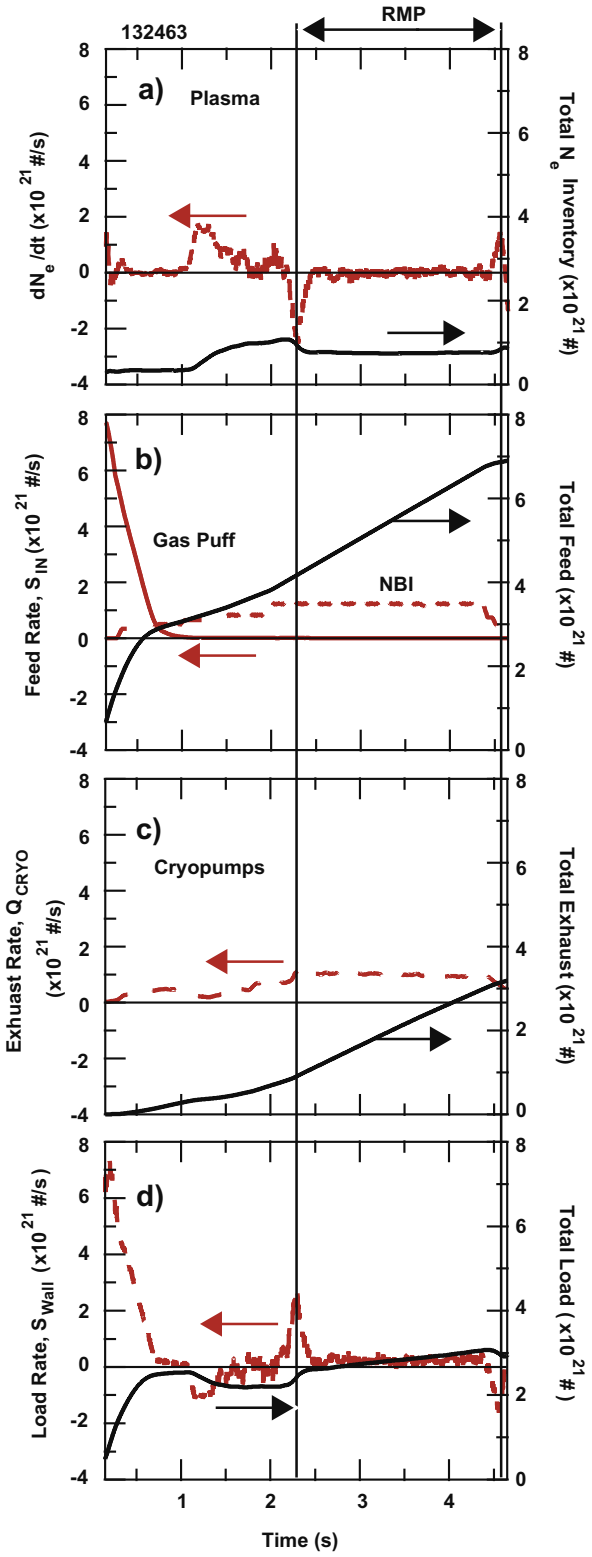

Fig. 2. Output of a D_2 particle balance of an RMP shot; (a) core plasma particle rate of change, dN_e/dt, on the left-hand axis and total inventory, N_e, on the right-hand axis; (b) particle input rate, S_{IN}, due to either the gas puff or NBI on the left-hand axis and the total input particles due to gas puff and NBI on the right-hand axis; (c) exhaust rate, Q_{cryo}, on the left-hand axis and the total particles exhausted due to the cryo-pumps on the right-hand axis and (d) wall load rate, S_{wall}, on the left-hand axis and total particles in the wall on the right-hand axis.

The particle balance analysis discussed in the previous paragraphs allows for a calculation of the particle decay rate,

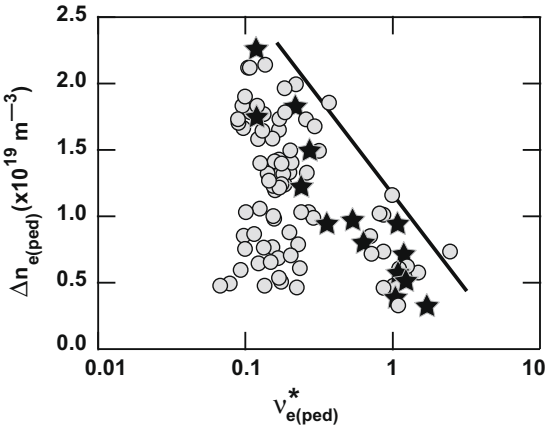

Fig. 3. Comparison of the pump-out magnitude, Δn_e, to the collisionality at the pedestal, $\nu^*_{e(ped)}$. The line is only to guide the reader's eye and each point is for an individual RMP discharge. Symbols marked (★) are given to indicate discharges used in later analysis, see Fig. 5.

$\tau^*_p = N_e \cdot (dN_e/dt - S_{IN})^{-1}$ [14]. This gives a relative calculation of the effects of wall retention and active pumping. Fig. 4 shows the time history of τ^*_p for a high-$\nu^*_{e(ped)}$ and a low-$\nu^*_{e(ped)}$ discharge for the time period spanning the RMP, as indicated by the I_{coil} current bar near the bottom of the graph. For both the high- and low-$\nu^*_{e(ped)}$, $\tau^*_p = 1.7$ s prior to the I_{coil} turn-on. After the I_{coil} turns on, there is a transient drop in τ^*_p to ~0.25 s for the low-$\nu^*_{e(ped)}$, and to 1.2 s for the high-$\nu^*_{e(ped)}$ case. This transient is coincident with the pump-out in n_e. After this transient in the low-$\nu^*_{e(ped)}$ case, τ^*_p approaches ~0.4 s which is ~1/4 of the pre-I_{coil} value and in the high-$\nu^*_{e(ped)}$ case τ^*_p returns to the initial value of ~1.7 s. Finally, after the I_{coil} turns off the low-$\nu^*_{e(ped)}$ case returns to the pre-I_{coil} value, whereas the high-$\nu^*_{e(ped)}$ case increases slightly before again returning to ~1.7 s.

Since the τ^*_p calculation is effectively equivalent to the particle balance shown in Fig. 2, we can interpret the large drop in τ^*_p (~a factor of 4) for the low-$\nu^*_{e(ped)}$ case shown in Fig. 4 to be due to a strong effect from the walls (e.g. from surfaces newly wetted because of the RMP). A more detailed 2D or 3D analysis, taking into account the fueling and pumping efficiency and wall recycling, is needed to determine if the n_e pump-out is indeed dominated by the wall retention or an otherwise transient increase in the SOL/divertor particle content [15].

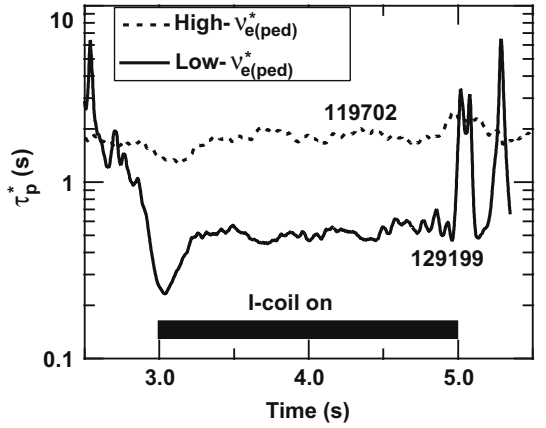

Fig. 4. Time history comparison of τ^*_p from (2) discharges. One has high-$\nu_{e(ped)}$ (119702) and the other has low-$\nu^*_{e(ped)}$ (129199). The time-base has been normalized to the I_{coil} turn-on for 129199.

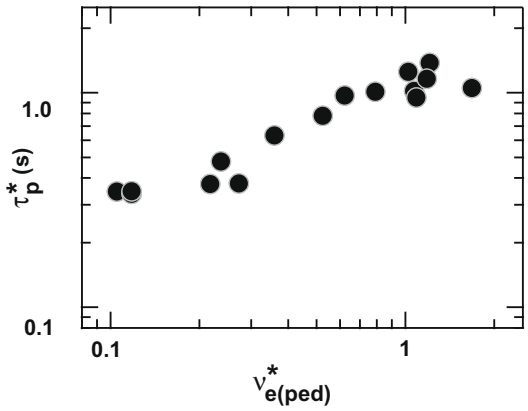

Fig. 5. Comparison of τ_p versus $v_{e(ped)}$ during the pump-out phase of a number of RMP discharges.

Finally, the initial transient drop in τ_p^* is correlated to the $v_{e(ped)}^*$ during the density pump-out phase. This correlation is shown in Fig. 5 as an increase in τ_p^* with increasing $v_{e(ped)}^*$ for a number of RMP discharges. The points on this figure are a subset of those in Fig. 3 (i.e. those points marked with a ★). It can be inferred from this figure that there is a less significant sink due to the wall/SOL as $v_{e(ped)}^*$, and implicitly n_e, increases. Since at higher $v_{e(ped)}^*$, there is a usually a larger wall load before the RMP begins as calculated from the particle balances. This figure suggests that as this sink is minimized (e.g. from more saturated walls), it has a smaller contribution to the change in τ_p^* during the RMP turn-on. This is also consistent with the large n_e pump-out magnitude at lower $v_{e(ped)}^*$ shown in Fig. 3.

3. Conclusions and summary

In this paper we present a systematic study of the pump-out phase in DIII-D RMP discharges. It is shown that the pump-out magnitude, Δn_e, measured in a large collection of discharges has an upper envelope that is inversely proportional to $v_{e(ped)}^*$ in DIII-D discharges starting with well-depleted walls. Particle decay times are calculated based on global D_2 particle balances and show an increase in τ_p^* as $v_{e(ped)}^*$ increases. This observation is consistent with the pump-out magnitude results and also factors in possible contributions from wall retention and/or active pumping. Both results suggest that the underlying physics mechanism of the density pump-out could be an increase in edge particle transport and/or that depleted walls are providing an additional sink due to newly wetted surfaces from the RMP topology. The full effects of the walls on the pump-out magnitude during an RMP is still under study but could be a factor in determining the performance of this ELM control technique in future long-pulse, burning-plasma devices (e.g. ITER) where particle exhaust control is a more serious issue due to wall retention concerns.

Acknowledgments

This research was supported by the US Department of Energy Fusion Energy Postdoctoral Research Program, administered by the Oak Ridge Institute for Science and Education under DE-AC05-06OR23100 and by the US Department of Energy under DE-FC02-04ER54698, DE-AC52-07NA27344, DE-AC05-00ER22725, DE-FG03-07ER54917, and DE-AC04-94AL85000.

References

[1] A. Loarte et al., Plasma Phys. Control. Fusion 45 (2003) 1549.
[2] T.E. Evans et al., Nucl. Fusion 45 (2005) 595.
[3] T.E. Evans et al., Nature Phys. 2 (2006) 665.
[4] S.C. McCool et al., Nucl. Fusion 30 (1990) 167.
[5] Ph. Ghendrih, A. Grosman, H. Capes, Plasma Phys. Control. Fusion 38 (1996) 1653.
[6] M. Greenwald et al., Nucl. Fusion 28 (1988) 2199.
[7] T.E. Evans et al., Nucl. Fusion 48 (2008) 024002.
[8] R.A. Moyer et al., Phys. Plasma 12 (2005) 056119.
[9] K.H. Burrell et al., Plasma Phys. Control. Fusion 47 (2005) B37.
[10] J.G. Watkins et al., J. Nucl. Mater. 363–365 (2007) 708.
[11] R. Maingi et al., Nucl. Fusion 36 (1996) 245.
[12] G.D. Porter, the DIII-D Team, Phys. Plasma 5 (1998) 4311.
[13] M.Z. Tokar et al., Nucl. Fusion 48 (2008) 024006.
[14] G.M. McCracken et al., Nucl. Fusion 33 (1993) 1409.
[15] R.R. Weynants et al., Nucl. Fusion 32 (1992) 837.